D5

N84 15595

# ORTHOTROPIC HOLE ELEMENT

J. W. Markham
Lockheed-Georgia Company

C. V. Smith
Consultant
Georgia Institute of Technology

## SUMMARY

A finite element was developed to adequately represent the state of stress in the region around a circular hole in orthotropic material experiencing reasonably general loading. This has been achieved through a complementary virtual work formulation of the stiffness and stress matrices for a square element with a center circular hole. The element has been incorporated into COSMIC-NASTRAN as a "dummy" element. Sample problems have been solved and these results are presented.

## INTRODUCTION

Mechanical fastening is the most used joining method in present flight vehicle structures. This results in connection details that contain many circular holes. These connections are subjected to very general loading with the additional complications of load transfer through fasteners and the use of nonisotropic materials in the connection. Because of the high stresses in these areas, it is important that an accurate evaluation of the local stresses around each hole be obtained to evaluate the performance of the joint.

The finite element method is an effective way to treat problems with complex geometry, material, and loading. However, because of the complexity of the stress state around fastener holes, a large number of conventional elements would be required to provide an adequate representation of the hole neighborhood. This means the cost of the analysis, both in computer costs and man-hours, will be high.

A solution to this problem would be an efficient special purpose finite element which provides an accurate representation of the state of stress around a hole without the need for many conventional elements. This has been done previously for isotropic materials. In 1981, under a contract with NASA-Langley, Lockheed-Georgia Co. developed an orthotropic hole element (Ref. 1).

## ELEMENT GEOMETRY

The orthotropic hole element is considered to be a thin plate in a state of plane stress with displacements on the external boundary specified so as to insure displacement continuity with adjacent elements. The element is a variable-noded total element and is defined via ADUM7, CDUM7, and PDUM7 input cards into NASTRAN. The user may specify the number of nodes on each of the three boundaries as shown in Figure 1. The nodes on the exterior of the element have two cartesian degrees of freedom whereas the nodes on the hole wall have only a single radial degree of freedom. The ratio of element width to hole diameter is determined from grid point locations and is thus a user choice; however, a ratio of four is recommended. The material properties may be isotropic or orthotropic and are defined by MAT1 or MAT2 cards. Characteristics which are not defined for this element include mass properties, thermal loading, material nonlinearity, and differential stiffness.

## ELEMENT INPUT

A great deal of user flexibility has been retained in the input for this element. Defaults have been provided and therefore the input can be quite simple. The following input is required for the element:

- Total number of nodes
- Element and property identification
- Grid point connection
- Material identification
- Thickness

The following input is optional:

- Number of segments on each of the three boundaries
- Number of integration intervals per segment for each of the boundaries
- Number of Gaussian integration points per interval for boundary integration
- Number of integration intervals per volume octant
- Number of stress terms with powers of $r > -2$. Input for each of the four symmetry conditions.
- Number of stress terms with powers of $r < -2$. Input for each symmetry condition.
- Definition of stress output locations.

## ELEMENT ADVANTAGES

Use of the orthotropic hole element can result in a substantial savings in computer costs and manhours. Savings in computer costs can be obtained particularly with models containing multiple holes because the congruency feature of NASTRAN can be used conveniently. This means that several hole elements of similar geometry can be included in the model and the stiffness matrix is only generated once. For complex geometries involving conventional elements, the congruency feature is impractical.

Use of the hole element can also result in substantial savings in manhours. A single hole element can replace dozens or even hundreds of conventional elements, therefore reducing the time required for modeling. Typically, an orthotropic hole element can be defined with eight input cards, thus no data generators or preprocessors are required for these areas of the model. Another advantage that results in manhour savings is the stress output generated by the hole element. The user can obtain stress components at any location within the element. With a conventional model, obtaining stresses at desired locations can be a laborious task because of the need to manipulate data and because of the large number of elements involved.

## EXAMPLE PROBLEMS

The example problems which follow were solved with the COSMIC-NASTRAN program at Lockheed-Georgia Company with the orthotropic hole element implemented. They are intended to demonstrate the performance of the element in a variety of applications.

### Isotropic Plate with Uniaxial Tension

The orthotropic hole element can be used in isotropic applications by simply specifying isotropic elastic coefficients. This is demonstrated by presenting the solution for an infinite isotropic plate with unit uniaxial tension at infinity (see Figure 2). The finite element model is shown in Figure 3. The plate width is 20 times the hole diameter, which represents an essentially infinite plate. Poisson's ratio is set at 0.3205.

Table 1 presents results for the three stress components at four values of radius and four values of $\theta$. The hole element stiffness and stress matrices were based on a geometry of 8 exterior nodes and 12 interior nodes (on the hole boundary). The hole boundary is given by $r = 1$. Note the excellent satisfaction of the zero radial stress boundary condition; the results were typically $10^{-6}$ times the magnitude of external loading. The circumferential stress results are also very good, with an error of only 0.2% on the maximum tension stress concentration factor and 1.5% on the maximum compression stress. The zero shear stress condition is perfectly satisfied since it was included in the original stress assumptions.

The stresses away from the hole boundary are also very well represented by the hole element results.

## Isotropic Plate with Half Cosine Loaded Hole

A load transfer problem for which a comparison solution is available (Ref. 3) is that of an infinite isotropic plate with Poisson's ratio equal to 0.25, loaded with uniform traction on one end and a cosine variation of radial tractions on the hole boundary (see Figure 4). The total load on the end is equal to 2P, and the radial tractions on the loaded hole boundary are given by

$$T_r = \frac{4P}{\pi} \cos\phi, \quad -\frac{\pi}{2} \leq \phi \leq \frac{\pi}{2}$$

The finite element model is shown in Figure 3. Table II presents results for the region around the hole, based on a geometry of 8 exterior nodes and 16 interior nodes. The value of P is set equal to 1.0.

Stresses at the hole boundary are very well represented by the finite element results. The radial stresses follow the cosine curve over the loaded region and are of the order of $10^{-2}$ on the unloaded portion of the boundary. The variation of circumferential stress is reasonably accurate, with an error of 3% on the maximum stress concentration.

In the region around the hole, the results from the hole element solution continue to give a good description of the stress state.

## $\pm 45^{\circ}$ Laminated Plate

The example problems with isotropic material serve to confirm the basic theoretical approach and to partially validate the computer solution. There remains to demonstrate satisfactory performance in applications with orthotropic materials. The first material selected has material properties as follows:

$$E_x = E_y = E, \quad G_{xy} = 1.697528E, \quad \nu_{yx} = \nu_{xy} = 0.735$$

Note that even though $E_x = E_y$, this material is rather "far" from isotropic, with some unspecified measure, due to the large value of Poisson's ratio and the fact that E, G, and $\nu$ do not satisfy the isotropic relationship. These properties describe the $\pm 45^{\circ}$ graphite/epoxy laminate considered in Reference 4.

The first loading is unit tensile tractions in the y-direction, applied as shown in Figure 2 with the finite element model given in Figure 3. The computed radial stresses at the hole boundary were of the order $10^{-6}$ times the exterior loading thus satisfying traction boundary conditions. Figure 5 shows the variation of circumferential stress around the hole boundary for a hole element geometry consisting of 8 exterior nodes and 12 interior nodes. Also shown is the exact solution for an infinite plate, given by

$$\tau_\theta = \frac{3.05786 \cos^2 \theta - 1}{2.8809072(\cos^4 \theta - \cos^2 \theta) + 1}$$

which can be deduced from Reference 5, p. 175. The orthotropic hole element results contain the essential feature that the maximum stress concentration does not occur at the familiar location of $\theta = 0^\circ$. The error in maximum stress is only 0.7%.

The hole loaded with half-cosine distributed tractions has also been solved; see Figure 4. The resulting radial stresses on the boundary are essentially identical to the results achieved in the case of isotropic material. The maximum circumferential stress on the hole boundary is $\tau_\theta = 0.79$ at $\phi = 125^\circ$, which can be compared with the hole element results for isotropic material of $\tau_\theta = 0.84$ at $\phi = 85^\circ$. Again, it is seen that the location of maximum stress has shifted around the circle from the familiar location.

Plywood

The next material selected has properties as follows:

$$E_y = E, \quad E_x = 2E, \quad G_{xy} = 0.11667E, \quad \nu_{xy} = 0.036$$

These properties describe a plywood material for which Reference 5 contains many results for an infinite plate. Note that the plywood properties are quite different from the $\pm 45^\circ$ lamination properties, both in magnitudes and relationships. This provides further checks on the ability of the hole element to handle different types of orthotropic material.

The types of loading considered are unit tensile tractions in the y-direction (Figure 2), unit compressive tractions in the x-direction with constraint in the y-direction (Figure 6a), and uniform unit internal pressure on the hole boundary (Figure 6b). For all cases, the finite element model is shown in Figure 3; and the element geometry contains 8 exterior nodes and 24 interior nodes.

For the uniaxial tension, there is the usual excellent satisfaction of traction boundary condition, with $\tau_r$ of the order $10^{-6}$. Circumferential stresses around the hole boundary are shown in Figure 7. Also shown are the exact results for an infinite plate, given by

$$\tau_\theta = \frac{4.8557 \cos^2 \theta - 0.7071}{-6.9994 \cos^4 \theta + 7.4994 \cos^2 \theta + 0.5}$$

which can be deduced from Reference 5 p. 175. The general features of the variation of stress are demonstrated by the hole element results.

The constrained compression results satisfy the hole boundary conditions, with $\tau_r$ of the order $10^{-5}$. Circumferential stresses around the boundary are shown in Figure 8. The exact results for infinite plate are given by

$$\tau_\theta = \frac{1.1155 - 6.5174 \sin^2\theta}{-13.9989 \sin^4 \theta + 12.9989 \sin^2 \theta + 2}$$

deduced from Reference 5 p. 179.

The internal pressure results provided boundary radial stresses of the magnitude -1.00002, which is again excellent satisfaction of boundary conditions. Circumferential stresses around the boundary are shown in Figure 9, compared to infinite plate exact results given by Reference 5 p. 173.

$$\tau_\theta = \frac{4.8829 - 15.8432 \sin^2 \theta + 13.9989 \sin^4\theta}{2 + 12.9989 \sin^2\theta - 13.9989 \sin^4\theta}$$

## Orthotropic Laminates with Pin-Loaded Holes

A class of problems which is of particular interest to the aircraft industry is that of pin-loaded holes in orthotropic laminates. Finite element solutions for a variety of graphite epoxy laminates were presented by Crews (Ref. 6). The finite element model used for these analyses was quite detailed, as shown in Figure 10. These results are used here as a basis of comparison to results obtained using the orthotropic hole element.

A NASTRAN model was constructed as shown in Figure 11. The particular case presented here is for W/d = 20. The load is applied at the center of the fastener and is reacted on both edges of the model in order to more closely approximate an infinite sheet. A feature of Lockheed-Georgia's version of COSMIC-NASTRAN was invoked to properly account for the contact area of the fastener. The hole element geometry consisted of 16 exterior nodes and 20 interior nodes. Six different laminates were considered. These were (1) quasi-isotropic (2) $0^\circ$ (3) $90^\circ$ (4) $[0^\circ/90^\circ]_s$ (5) $[\pm 45^\circ]_s$ and (6) $[0^\circ/\pm 45^\circ]_s$. Figures 12-17 present plots of the tangential and radial stress components obtained by the hole element for these respective materials in comparison to the results obtained by Crews using a detailed classical model.

These plots indicate that a reasonable correlation was obtained for the tangential stress distribution at the hole boundary. Peak tangential stress differed by no more than 12%. Excellent correlation of radial stress distribution was obtained for all cases.

## Multiple Holes

Figure 18 shows a finite element model of a plate containing five holes. For economy in modeling, it is desirable to develop the hole element stiffness matrix only once and then transform this matrix as necessary to represent all the hole elements. This is possible in NASTRAN by using the congruency feature, and this feature has been checked by determining the solution to Figure 18 with tension applied parallel to the row of holes. The material is isotropic with Poisson's ratio of 0.3205.

The maximum stress concentration factor is given in Reference 7, p. 194 for an intermediate hole in an infinite row of holes. In order to simulate the infinite row, the displacements of each loaded end of the model were constrained to be uniform across the width of the plate. The finite element result for stress concentration is 2.78, based on a hole element geometry containing 8 exterior nodes and 12 interior nodes. Reference 7 gives 2.65; there is a 5% difference in results.

## Concluding Remarks

The performance of the orthotropic hole element in solving a variety of problems has demonstrated that it can produce acceptable results with significant advantages in computer costs, model preparation time, and post-processing of data. Even though the emphasis in this paper has been on problems concerning fastener holes, the use of this element is applicable to any isotropic or orthotropic plate containing circular holes.

TABLE 1

STRESSES FOR AN ISOTROPIC PLATE SUBJECTED TO UNIAXIAL TENSION

| | $\theta$ deg | $\tau_r$* | $\tau_r$** | $\tau_\theta$* | $\tau_\theta$** | $\tau_{r\theta}$* | $\tau_{r\theta}$** |
|---|---|---|---|---|---|---|---|
| r = 1 | 0 | 0 | 0 | 3.006 | 3.000 | 0 | 0 |
| | 30 | 0 | 0 | 2.005 | 2.000 | 0 | 0 |
| | 60 | 0 | 0 | -0.006 | 0 | 0 | 0 |
| | 90 | 0 | 0 | -1.015 | -1.000 | 0 | 0 |
| r = 2 | 0 | 0.279 | 0.281 | 1.221 | 1.219 | 0 | 0 |
| | 30 | 0.327 | 0.328 | 0.923 | 0.922 | 0.572 | 0.568 |
| | 60 | 0.422 | 0.422 | 0.325 | 0.328 | 0.571 | 0.568 |
| | 90 | 0.467 | 0.469 | 0.028 | 0.031 | 0 | 0 |
| r = 3 | 0 | 0.145 | 0.148 | 1.076 | 1.074 | 0 | 0 |
| | 30 | 0.295 | 0.296 | 0.815 | 0.815 | 0.516 | 0.513 |
| | 60 | 0.594 | 0.593 | 0.296 | 0.296 | 0.516 | 0.513 |
| | 90 | 0.739 | 0.741 | 0.031 | 0.037 | 0 | 0 |
| r = 4 | 0 | 0.083 | 0.088 | 1.036 | 1.037 | 0 | 0 |
| | 30 | 0.278 | 0.278 | 0.784 | 0.784 | 0.482 | 0.482 |
| | 60 | 0.659 | 0.659 | 0.284 | 0.278 | 0.488 | 0.482 |
| | 90 | 0.851 | 0.850 | 0.010 | 0.025 | 0 | 0 |

* Hole Element Results

** Reference 2

TABLE II

STRESSES FOR AN ISOTROPIC PLATE WITH LOAD TRANSFER

| | $\phi$ deg | $\tau_r$* | $\tau_r$** | $\tau_\theta$* | $\tau_\theta$** | $\tau_{r\theta}$* | $\tau_{r\theta}$** |
|---|---|---|---|---|---|---|---|
| r = 1 | 0 | -1.271 | -1.273 | 0.372 | 0.412 | 0 | 0 |
| | 30 | -1.099 | -1.103 | 0.467 | 0.470 | 0 | 0 |
| | 60 | -0.649 | -0.637 | 0.649 | 0.612 | 0 | 0 |
| | 90 | -0.041 | 0 | 0.834 | 0.810 | 0 | 0 |
| | 120 | -0.012 | 0 | 0.415 | 0.373 | 0 | 0 |
| | 150 | 0.003 | 0 | 0.056 | 0.053 | 0 | 0 |
| | 180 | 0.003 | 0 | -0.094 | -0.065 | 0 | 0 |
| r = 1.2 | 0 | -0.995 | -0.977 | 0.314 | 0.348 | 0 | 0 |
| | 30 | -0.844 | -0.829 | 0.358 | 0.381 | 0.035 | 0.021 |
| | 60 | -0.445 | -0.429 | 0.460 | 0.443 | 0.046 | 0.029 |
| | 90 | 0.038 | 0.034 | 0.477 | 0.415 | -0.032 | -0.031 |
| | 120 | 0.055 | 0.078 | 0.289 | 0.274 | -0.097 | -0.081 |
| | 150 | 0.023 | 0.038 | 0.070 | 0.088 | -0.064 | -0.051 |
| | 180 | 0.006 | 0.024 | -0.015 | -0.011 | 0 | 0 |
| r = 1.5 | 0 | -0.726 | -0.726 | 0.232 | 0.241 | 0 | 0 |
| | 30 | -0.604 | -0.609 | 0.256 | 0.253 | 0.042 | 0.026 |
| | 60 | -0.288 | -0.293 | 0.295 | 0.266 | 0.046 | 0.028 |
| | 90 | 0.045 | 0.037 | 0.266 | 0.231 | -0.047 | -0.045 |
| | 120 | 0.094 | 0.086 | 0.179 | 0.152 | -0.119 | -0.105 |
| | 150 | 0.055 | 0.049 | 0.062 | 0.055 | -0.083 | -0.070 |
| | 180 | 0.035 | 0.033 | 0.010 | 0.012 | 0 | 0 |

* Hole Element Results
** Reference 3

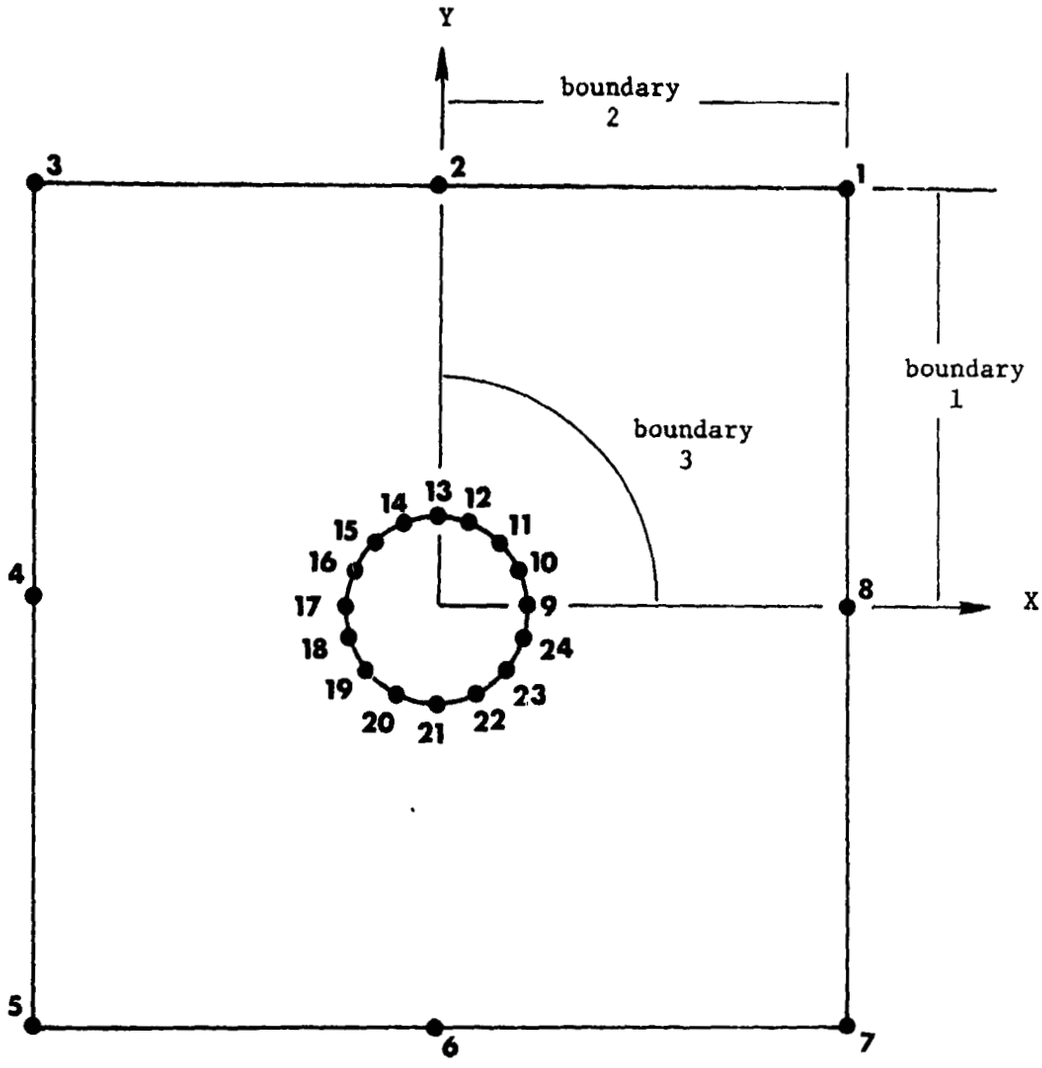


Figure 1. Orthotropic Hole Element Geometry

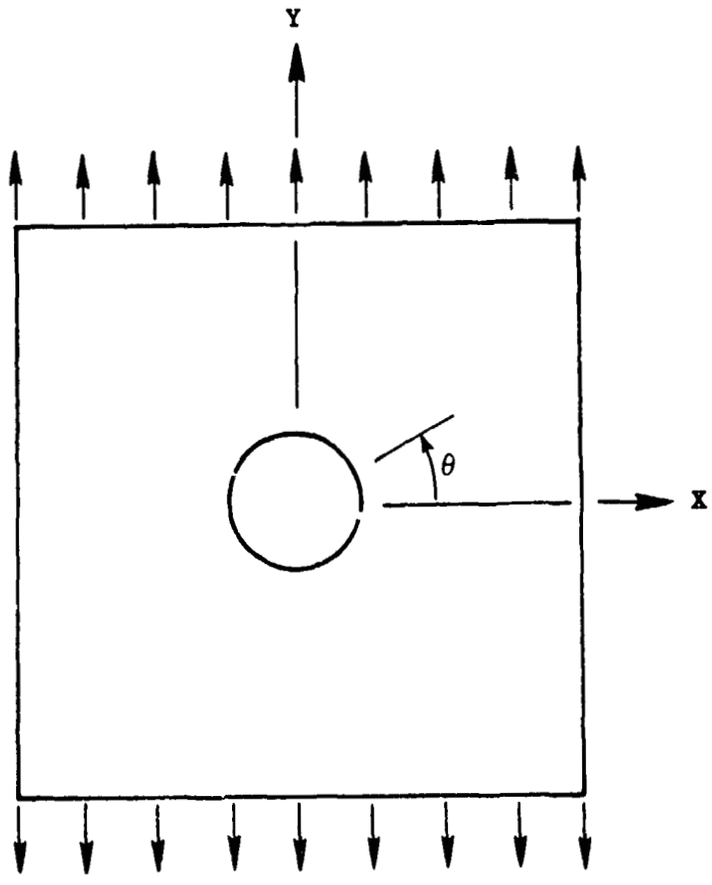


Figure 2. Unit Tensile Traction in the Y-Direction

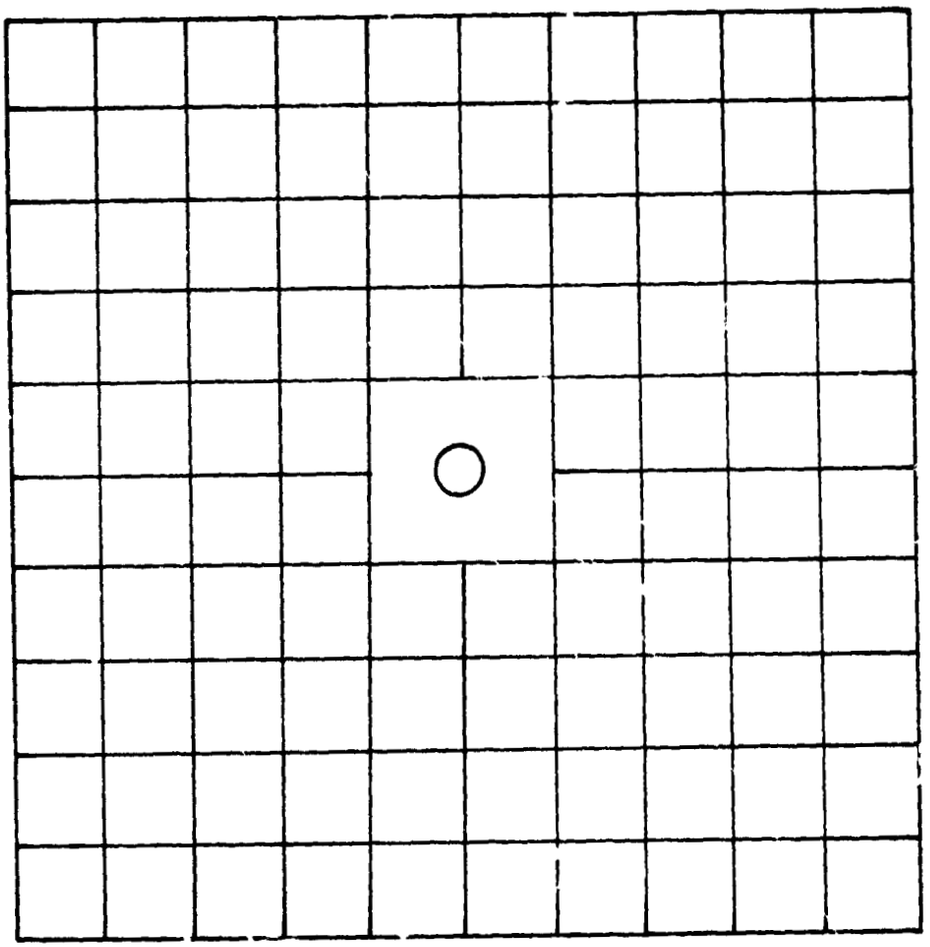

Figure 3. Finite Element Model

(b) Half Cosine Distribution of Traction on the Hole Boundary




(a) External Loading

Figure 4. Load Transfer Problem

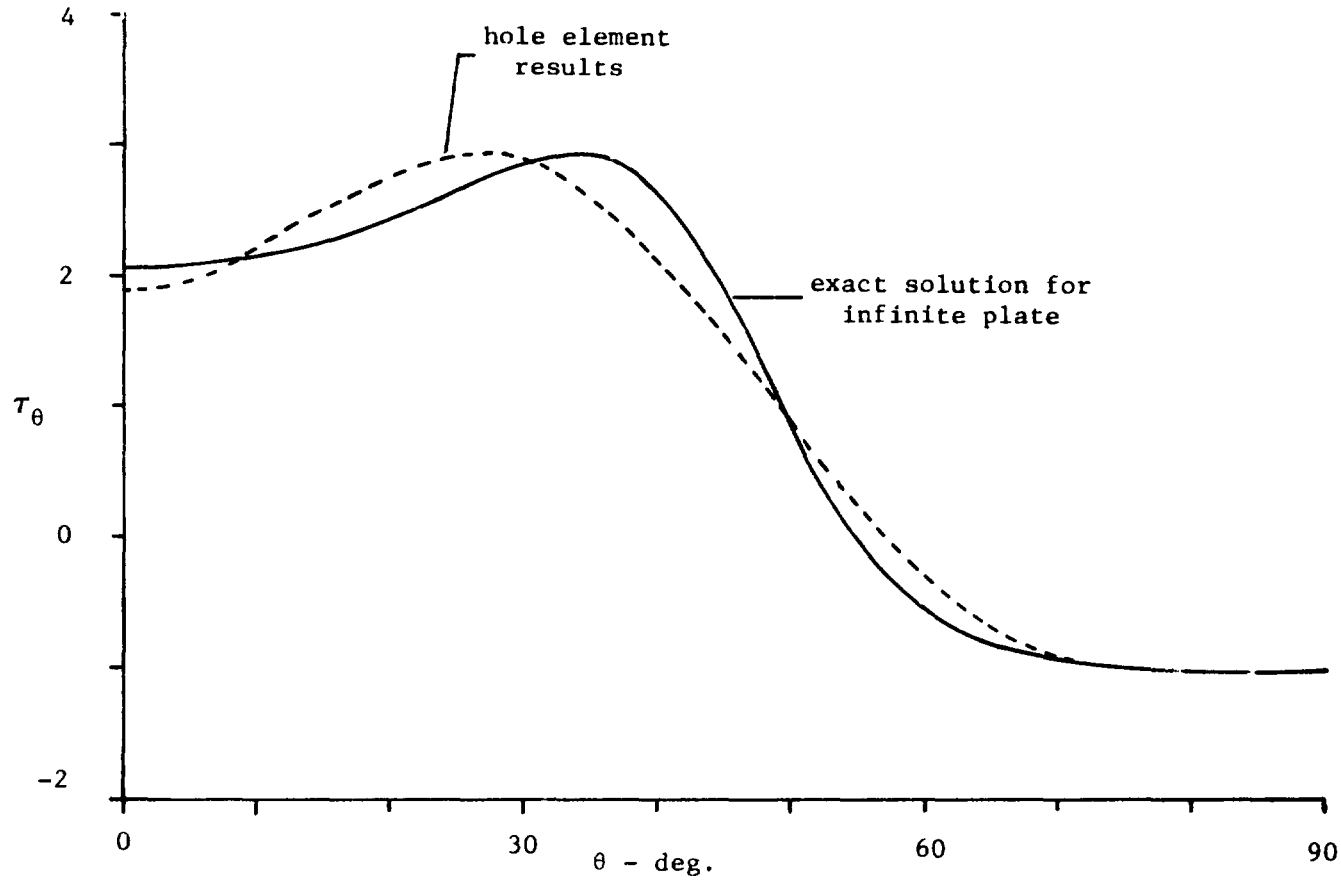






Figure 5. Circumferential Stress at the Open Hole Boundary for a $\pm 45^{o}$ Laminate with Unit Uniaxial Tensile Traction

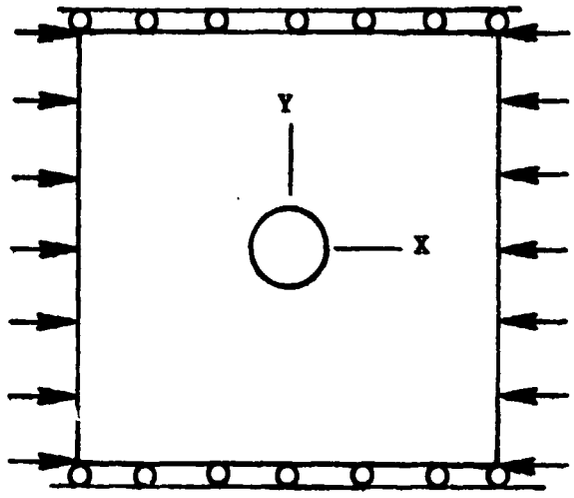


(a) Constrained Compression

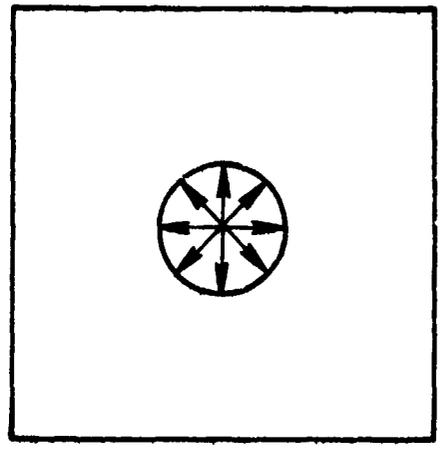

(b) Internal Pressure

Figure 6. External Loadings

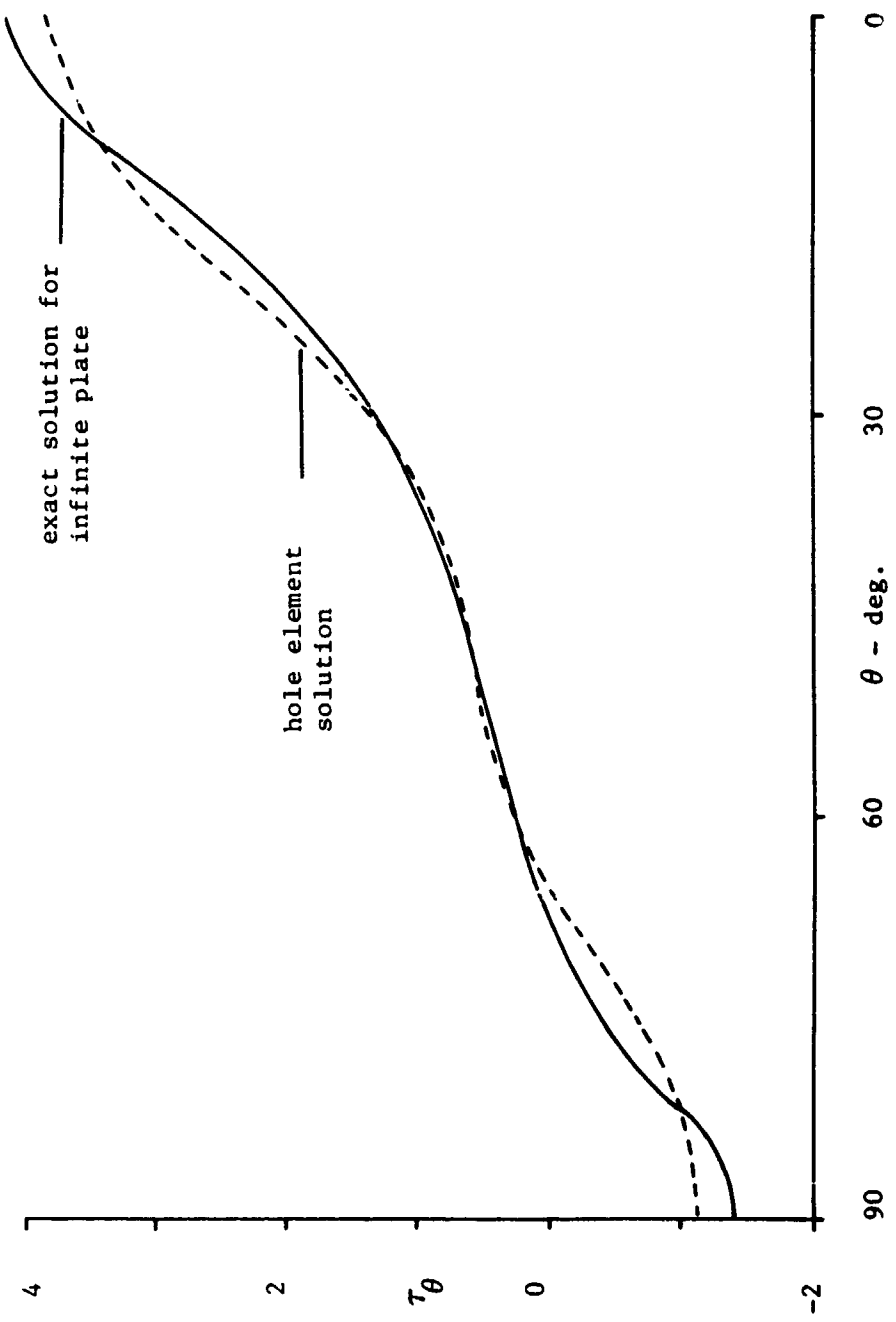


Figure 7. Circumferential Stress at the Open Hole Boundary for Plywood with Unit Uniaxial Tensile Traction

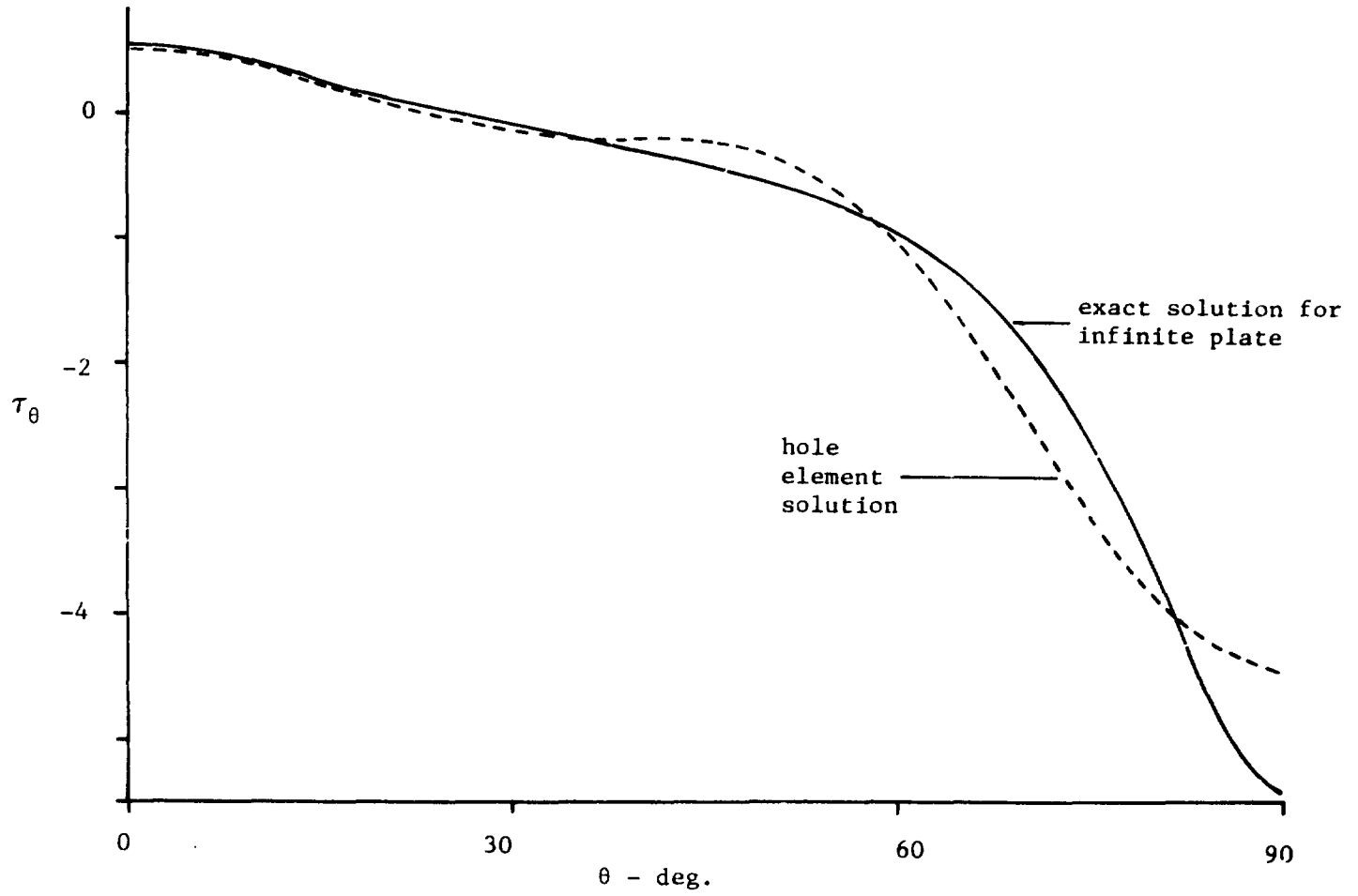


Figure 8. Circumferential Stress at the Open Hole Boundary for Plywood with Unit Constrained Compression

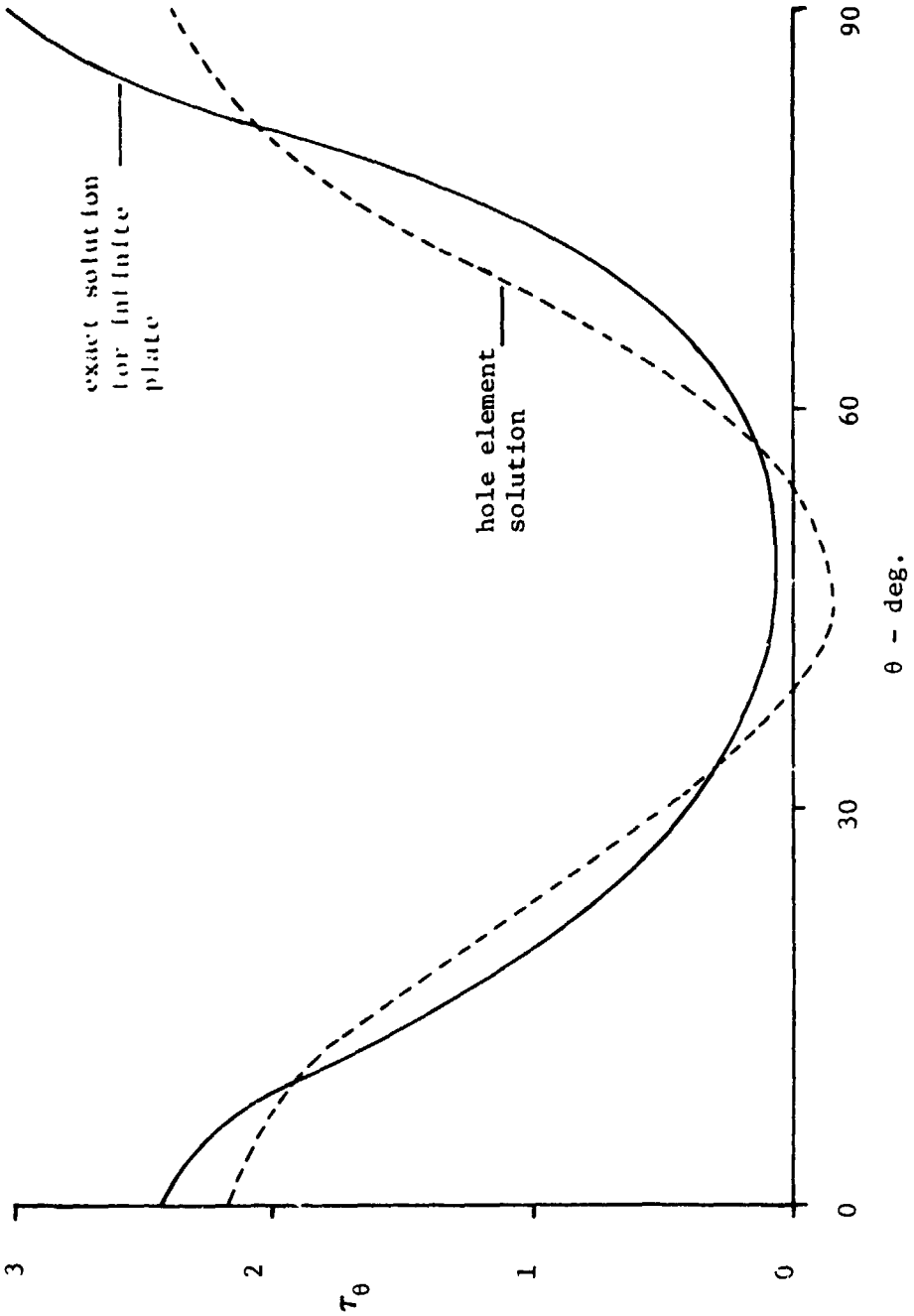


Figure 9. Circumferential Stress at the Hole Boundary for Plywood with Unit Internal Pressure on the Boundary

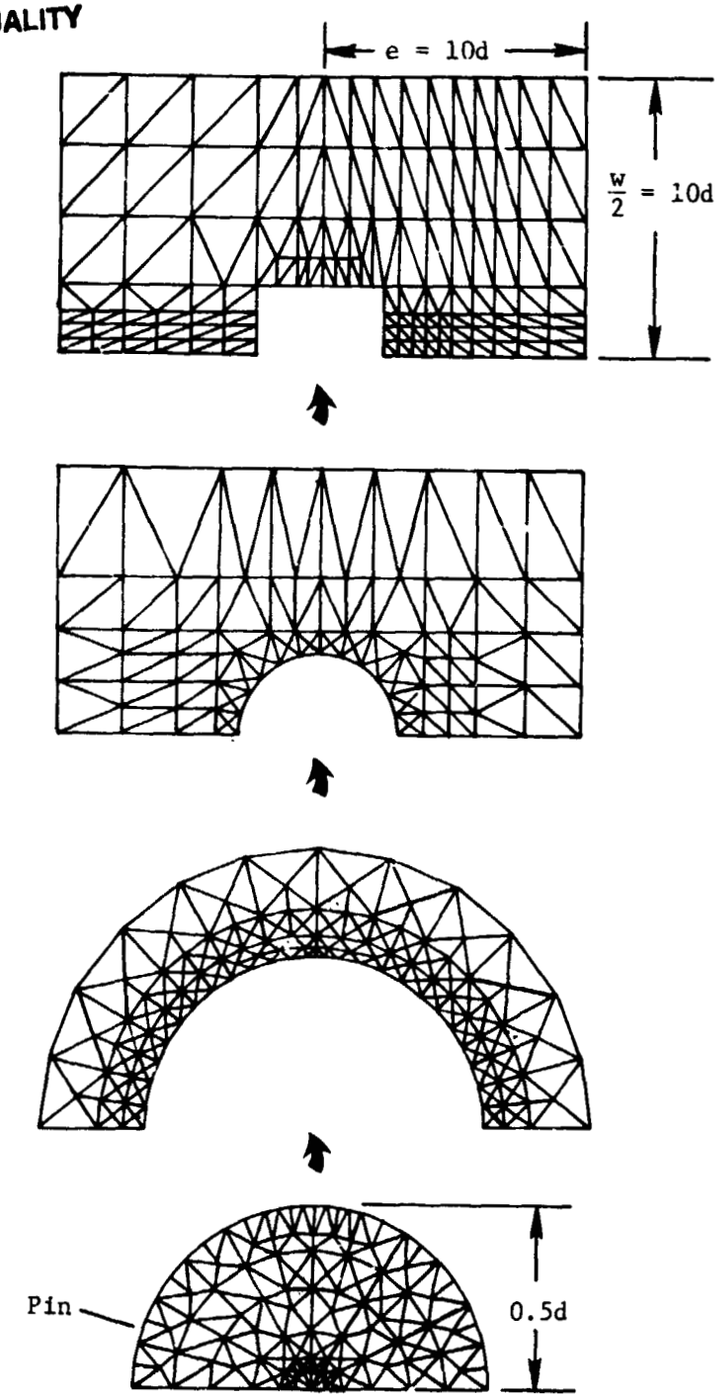


Figure 10. Detailed Finite Element Model for Analysis of Orthotropic Laminates with Pin-Loaded Holes

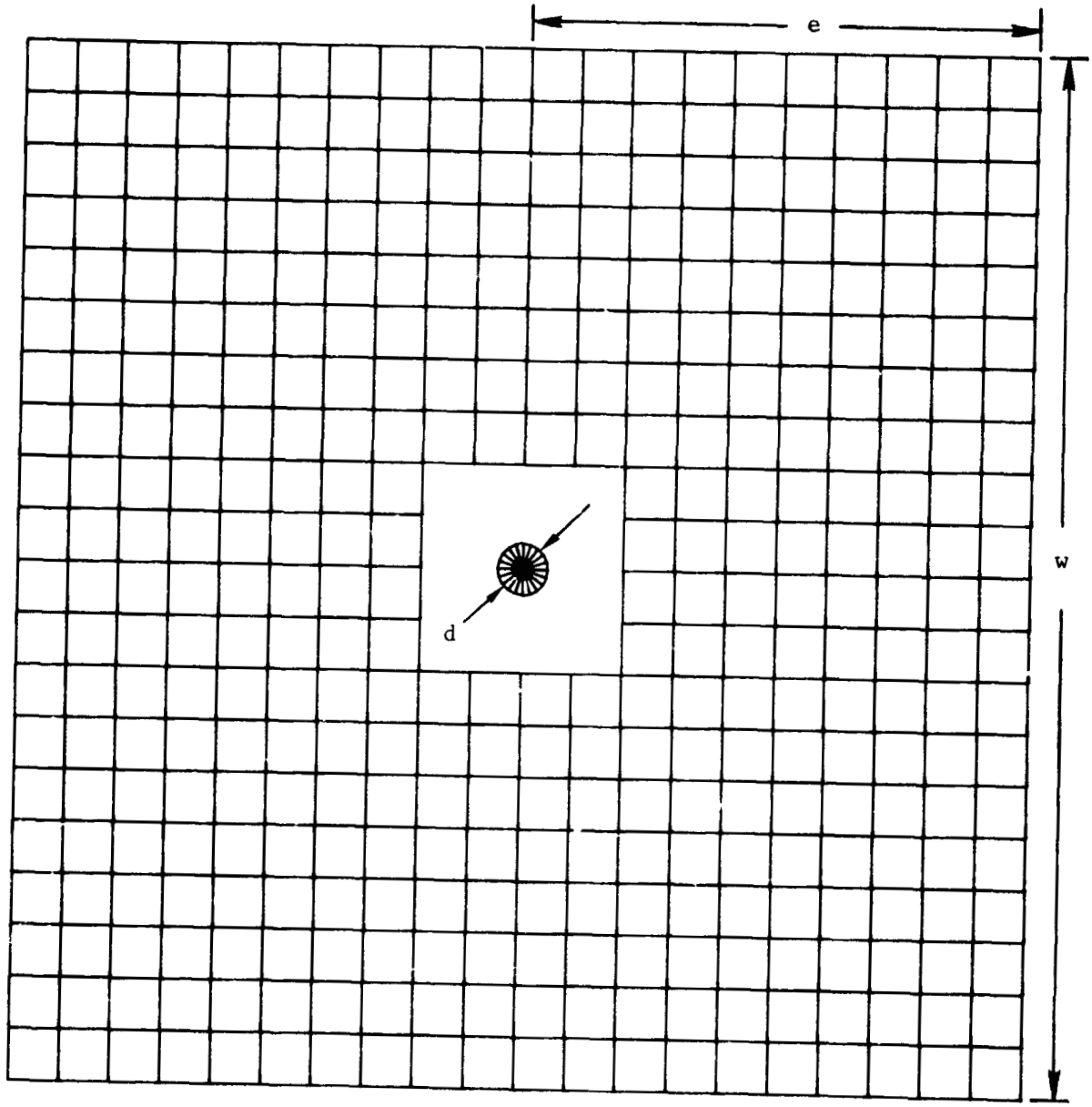


Figure 11. Finite Element Model with Hole Element

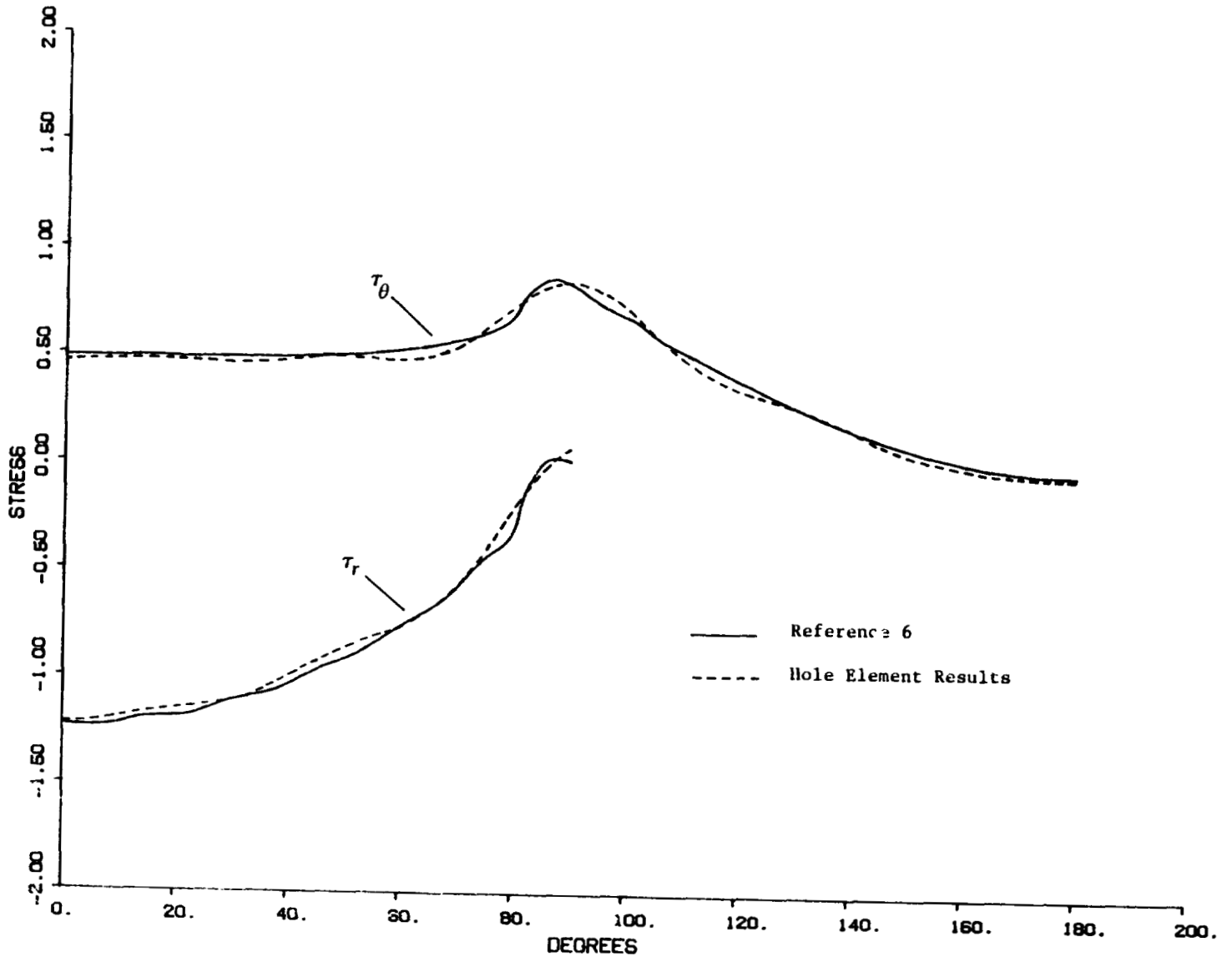


Figure 12. Stresses in the Quasi-Isotropic Laminate

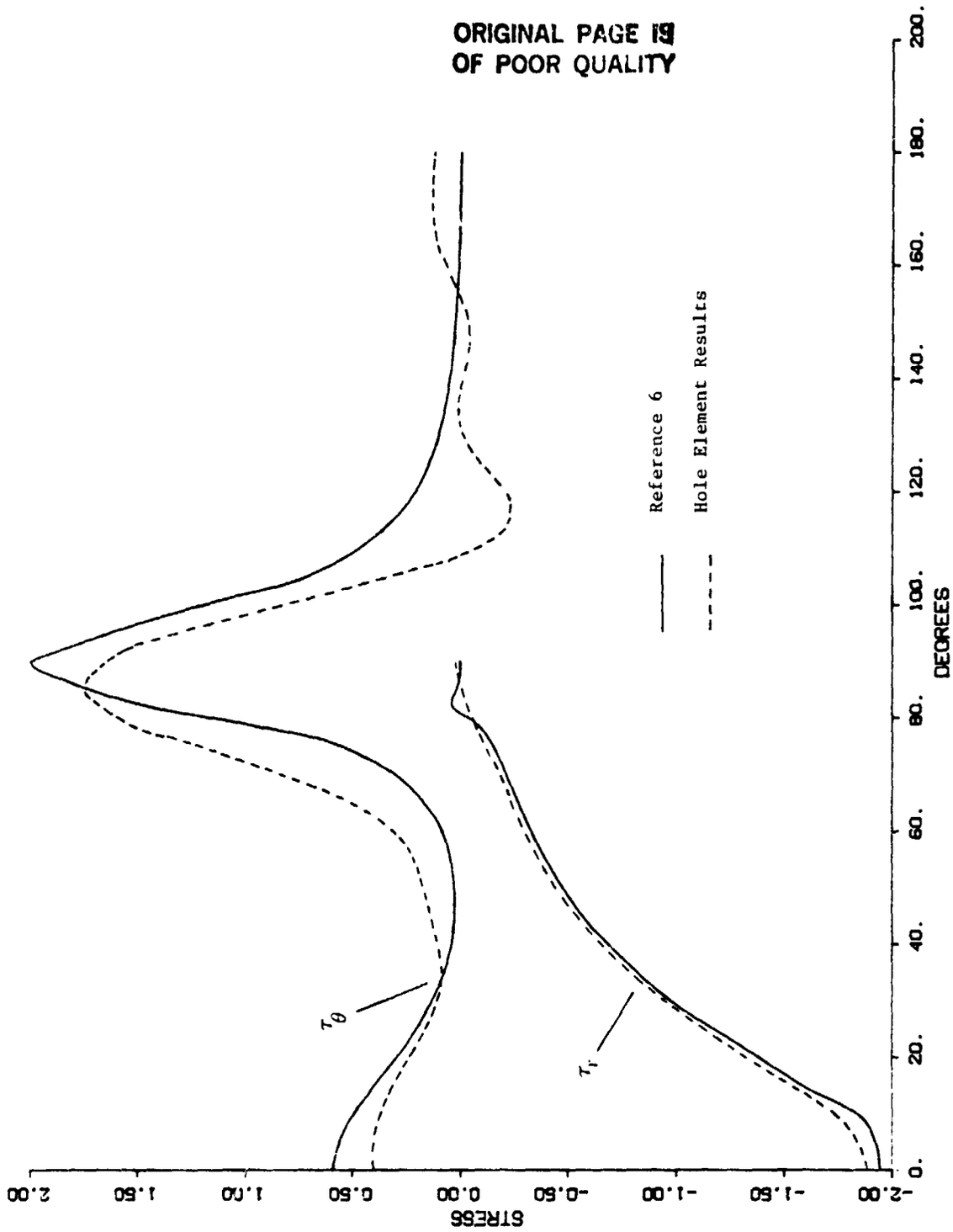


Figure 13. Stresses in the $0^0$ Laminate

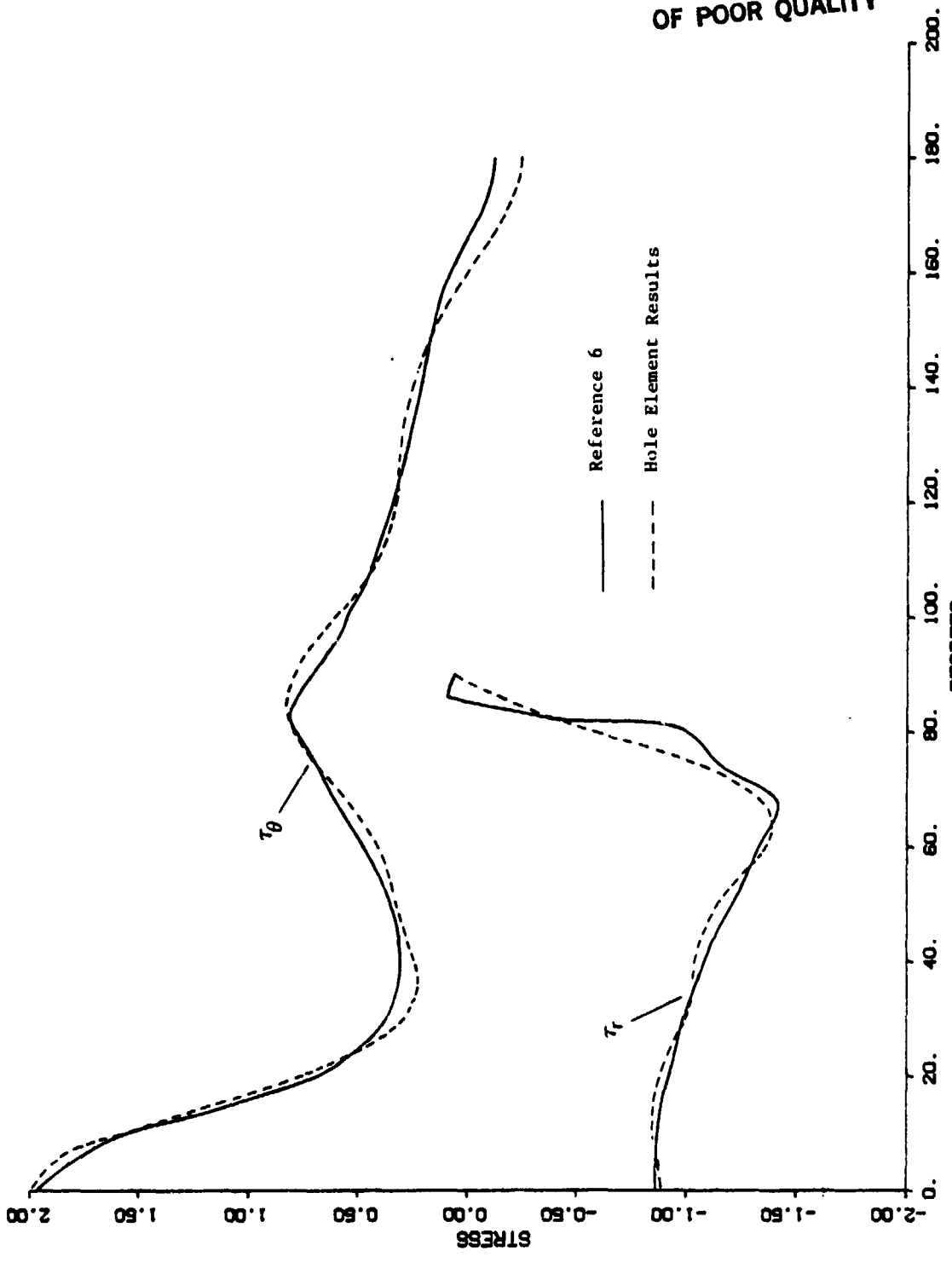


Figure 14. Stresses in the $90^{o}$ Laminate

ORIGINAL PAGE IS
OF POOR QUALITY

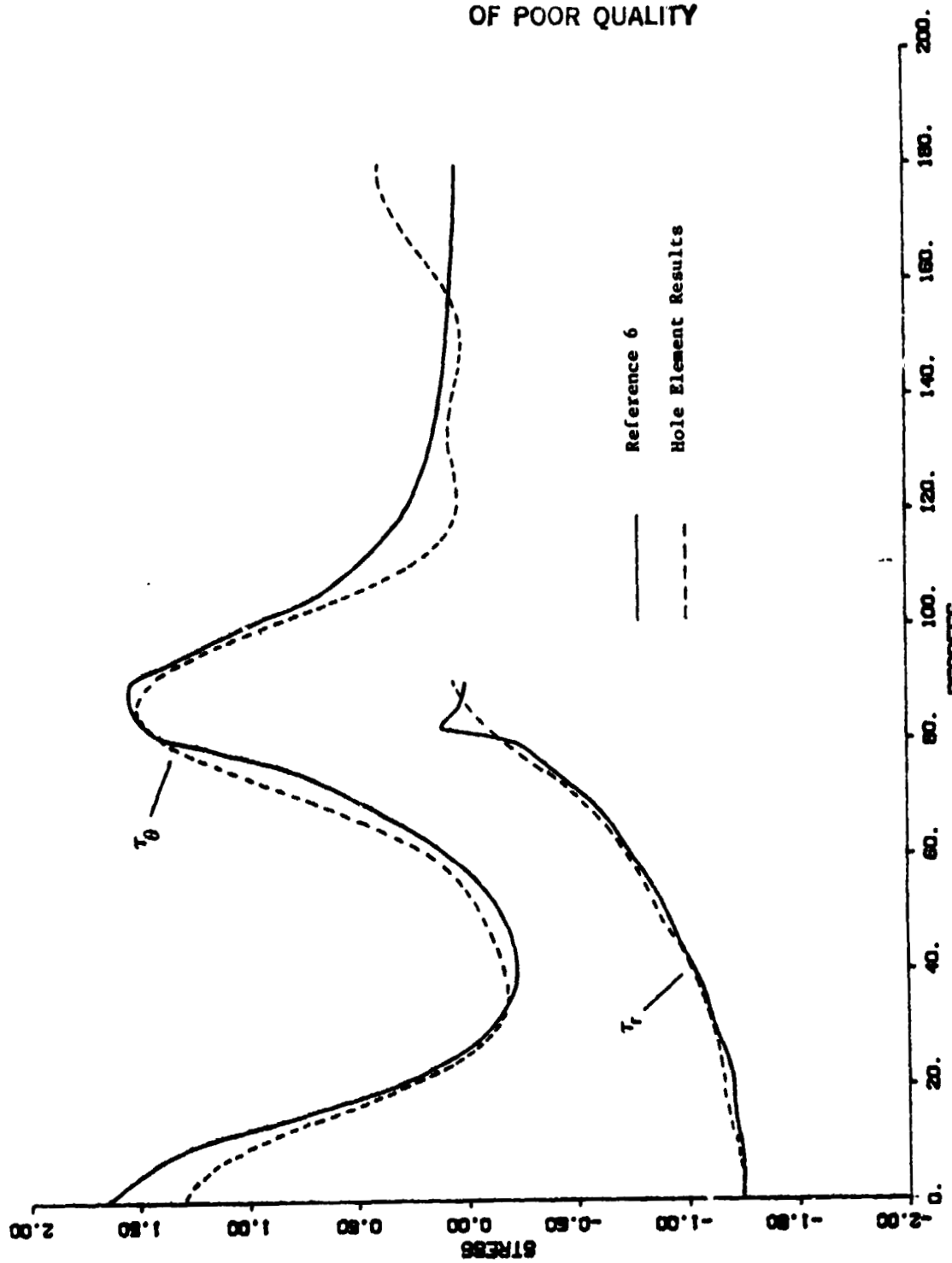


Figure 15. Stresses in the $[0^\circ, 90^\circ]_s$ Laminate

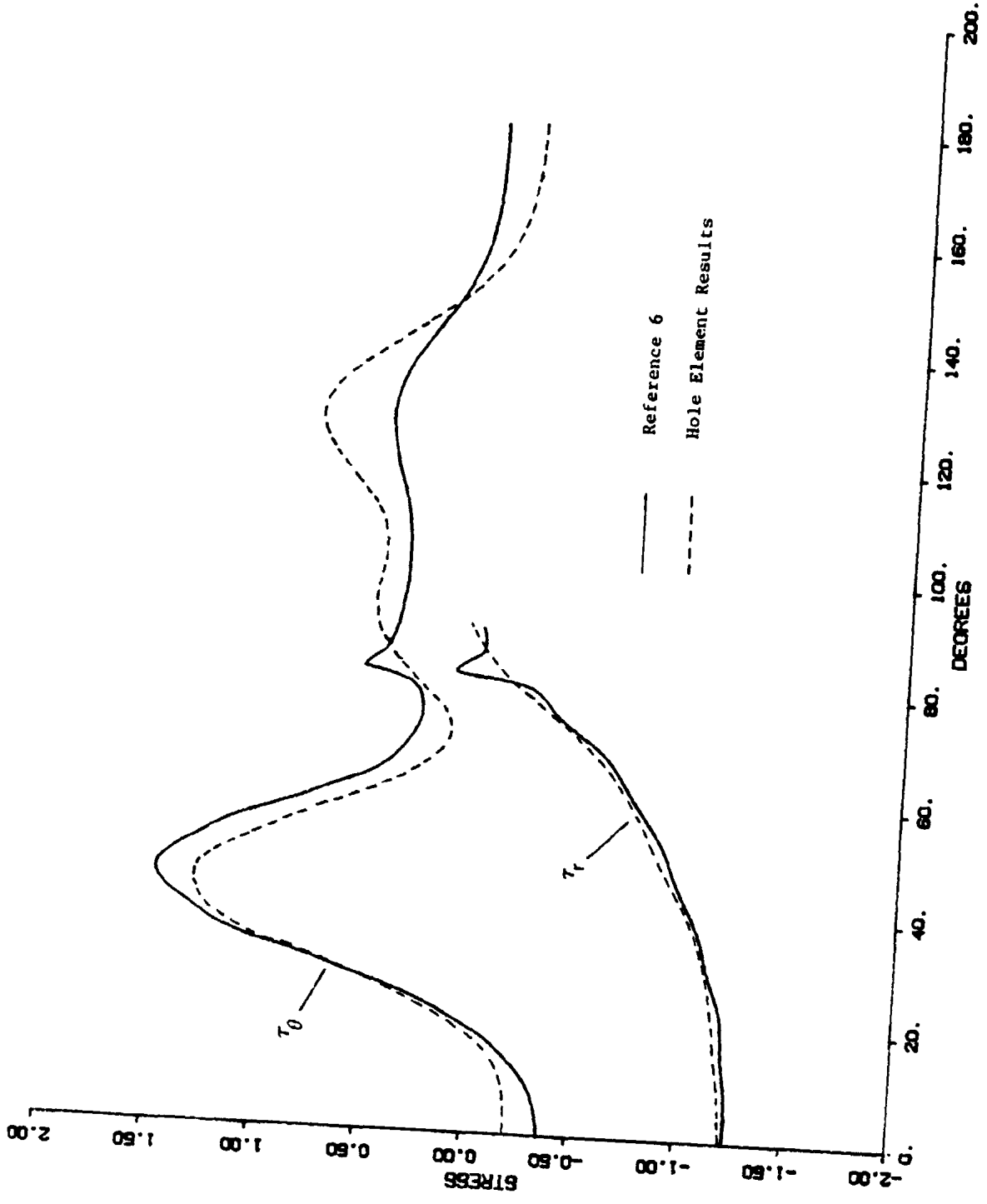


Figure 16. Stresses in the $[\pm 45^\circ]_s$ Laminate

Figure [illegible] Stress [illegible]

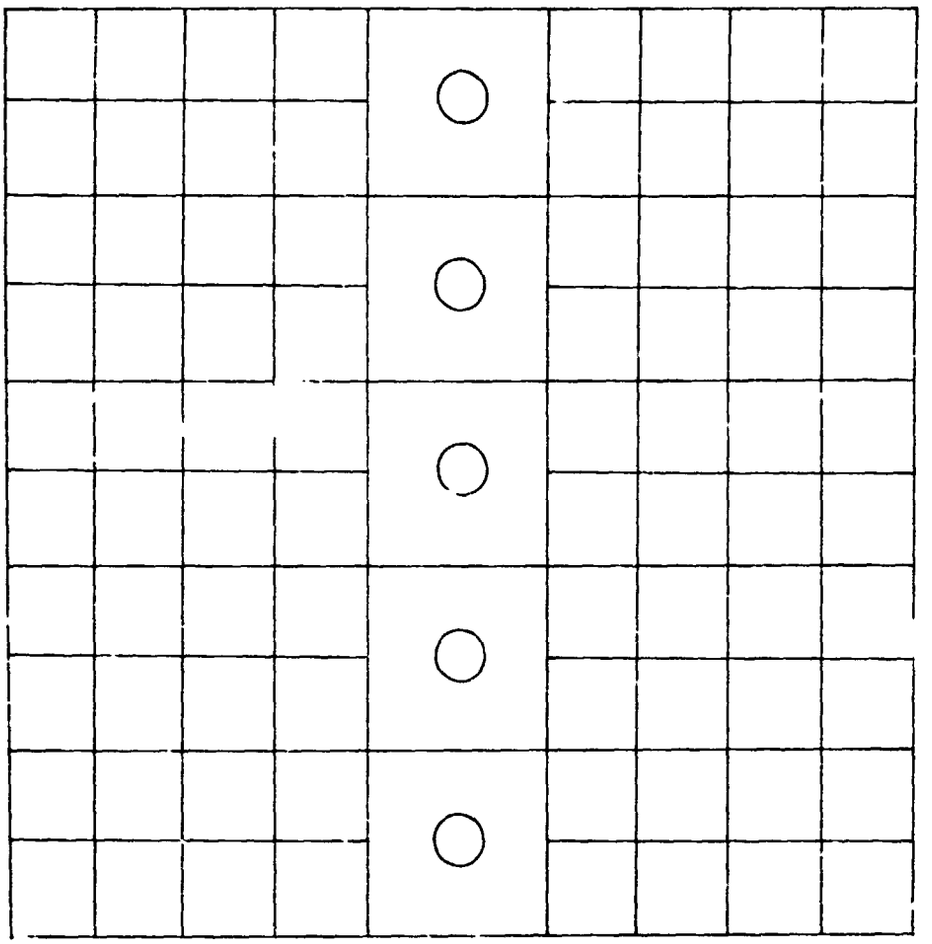

Figure 18. Finite Element Model for a Plate with Multiple Holes

## REFERENCES


1. Smith, C. V.; Markham, J. W.; Kelley, J. W.; and Kathiresan, K.: Development of an Orthotropic Hole Element. NASA CR165759, August, 1981.

2. Timoshenko, S. P.; and Goodier, J. N.: Theory of Elasticity. Third Edition, McGraw-Hill Book Company, New York, 1970.

3. Bickley, W. G.: The Distribution of Stress Round a Circular Hole in a Plate. Philosophical Transactions of the Royal Society of London, Series A , Vol. 227, 1928, pp. 383-415.

4. Hong, C. S.; and Crews, J. H.: Stress Concentration Factors for Finite Orthotropic Laminates with a Circular Hole and Uniaxial Loading. NASA TP1469, May, 1979.

5. Lekhnitskii, S. G.: Anisotropic Plates. Second Edition, Gordon and Breach, New York, 1968.

6. Crews, J. H.; Hong, C. S.; and Raju, I. S.: Stress-Concentration Factors for Finite Orthotropic Laminates with a Pin-Loaded Hole. NASA TP1862, May, 1981.

7. Peterson, R. E.: Stress Concentration Design Factors. John Wiley and Sons, New York, 1953.